



OPEN

Design and field experiment of *Codonopsis pilosula* film covering transplanter

Weining Luo¹, Wei Sun¹✉, Ming Zhao², Juanling Wang³ & P. A. Simionescu⁴

To address the low efficiency and high labor demands of manual *Codonopsis pilosula* cultivation, as well as the limitations of existing flat-type transplanting machines that create trenches of inconsistent depth hindering root growth and seedling emergence, a *C. pilosula* film-covered outcrop tilted transplanting machine was developed. Based on theoretical analysis of the prototype's key components and agronomic requirements for oblique *C. pilosula* transplanting, the structure and working parameters of the rotary tiller soil throwing device, soil lifting device, track-type soil conveying device, seedling throwing device, and film covering device were determined. The core components' working principles were analyzed, and the soil throwing process of the rotary tiller device was simulated using the discrete element method (DEM). A calculation domain was established, and the results showed that the average mass of the rotary tiller device was 49.44 kg, while the required soil lifting amount for the scraper-type soil lifting device was 21.84 kg, meeting the soil throwing requirements. Field experiments in 10 test areas demonstrated an average qualified rate of 89.50% for planting depth, 84.00% for planting posture, 90% for exposed plant spacing, 4.51 cm for plant spacing, and 8.67% coefficient of variation for planting spacing. These results meet industry standards for planting depth and planting spacing, confirming the machine's effectiveness in achieving high-quality tilted transplanting of *C. pilosula* seedlings.

Keywords Soil lifting device, Seedling feeding device, Drive system, Simulation analysis

Codonopsis pilosula has a long history of use in the traditional Chinese medicinal, praised for its ability to bolster the body's immunity, enhance appetite, and prevent diseases.

Gansu Province, a major production area of *Codonopsis pilosula* in China, has seen a steady increase in planting area, accounting for over 90% of the national production¹. As a significant economic crop in the region, *Codonopsis pilosula* provides a valuable source of income for local farmers. To retain moisture, and increase soil temperature, Gansu farmers have adopted a unique tilted planting model with exposed heads^{2,3}. This method, however, relies heavily on manual labor, highlighting the need for exploring more sustainable and efficient farming practices. The cultivation mode of artificial *Codonopsis pilosula* covered with plastic film and exposed heads is shown in Fig. 1.

Current transplanting machines primarily cater to bowl seedlings for vegetables, tobacco, and other crops, demanding a high degree of uprightness after planting^{4,5}. However, this approach falls short of meeting the agronomic requirements, movement trajectory, and planting posture needs for tilted transplanting of *Codonopsis pilosula*⁶.

Sweet potato and licorice are examples of crops requiring tilted transplanting techniques. While the existing belt-type mechanism for sweet potatoes employs an oblique approach⁷, its belt end could potentially damage *Codonopsis pilosula* seedlings. Furthermore, the morphology and agronomic needs of *Codonopsis pilosula* make this method unsuitable for its tilted transplanting with film covering.

Licorice transplanting utilizes a specialized trencher that controls soil particle flow to achieve tilted planting⁸. However, this method necessitates breaking the film and releasing seedlings later, making it less adaptable for *Codonopsis pilosula* tilted transplanting.

Crucially, the differing agronomic requirements of *Codonopsis pilosula* result in distinct trajectory and planting posture requirements compared to sweet potato and licorice⁹.

¹College of Mechano-Electronic Engineering, Gansu Agricultural University, Lanzhou 730070, China. ²Dingxi Sanniu Agricultural Machinery Manufacturing Co., Ltd, Dingxi 743000, China. ³Shanxi Agricultural University, Taiyuan 030031, China. ⁴Texas A&M University Corpus Christi, Corpus Christi, TX 78412, USA. ✉email: sunw@gau.edu.cn



Figure 1. Artificial *Codonopsis pilosula* covered with plastic film and tilted cultivation. (a) Artificial seeding. (b) Cover the seedlings with soil. (c) Covering the membrane edge and seedling with soil.

In China, mechanical equipment development for *Codonopsis pilosula* transplanting remains in its early stages. Existing machinery primarily focuses on flat-type transplanting, which suffers limitations due to its dependence on trench depth. Shallow trenches hinder root growth, while deep trenches impede seedling germination, leading to inconsistent emergence and unstable transplanting¹⁰.

Researchers have conducted various studies and innovations on the *Codonopsis pilosula* transplanter. The *Codonopsis pilosula* transplanter designed by Wenliang Dong et al.¹¹ can complete multiple tasks such as rotary tillage, fertilization, trenching, auxiliary seedling placement, soil shaping, film covering, and soil covering on the film. However, multiple manual assistance is required to complete the tasks, and the method of manually placing *Codonopsis pilosula* seedlings directly in the planting ditch while trenching is used, resulting in a relatively high seedling leakage rate. The ridge covered plastic film seed row covered soil *Codonopsis pilosula* seedling transplanting machine designed by Junzeng Wang et al.¹² uses a pointed and long winged trenching device to control soil backflow and complete soil burial, which improves the emergence rate, but also requires multiple manual assistance to complete the operation. In conclusion, current transplanting machines fail to satisfy the agronomic demands of film-covered tilted planting for *Codonopsis pilosula*.

The limitations of current *Codonopsis pilosula* flat transplanting machinery, including low seedling survival rates and unstable transplanting, necessitate the exploration of innovative transplanting methods and machinery^{13,14}. This paper proposes a novel *Codonopsis pilosula* exposed head tilted transplanting machine. This machine employs a trench opener to create a slanted planting trench. During planting, the seedling roots settle into the deeper side of the slope, while the tops rest on the shallower end, achieving a tilted planting effect. This addresses the challenge of inconsistent seedling emergence rates associated with flat transplanting machinery by ensuring consistent planting depth, ultimately enhancing the quality of *Codonopsis pilosula* seedling transplantation.

Overall structure and working principle

Agronomic requirements

Figure 2 depicts the planting mode for film-covered *Codonopsis pilosula* grown on outcrops with tilted cultivation, designed to meet the crop's agronomic requirements. *Codonopsis pilosula* seedlings, approximately 200 mm

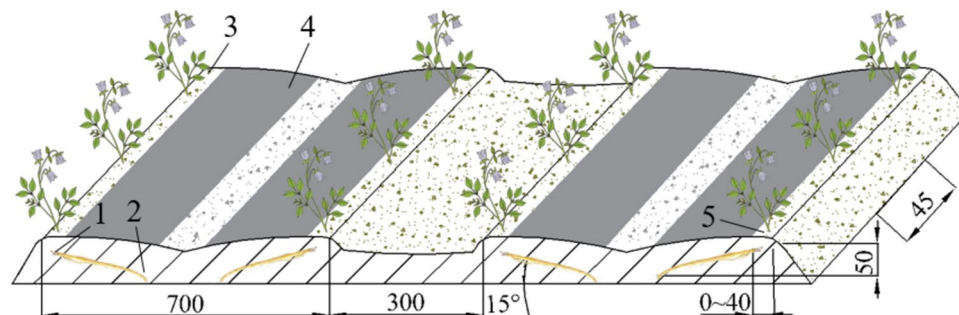


Figure 2. Diagram of the tilted cultivation mode of *Codonopsis pilosula*. 1. Root of *Codonopsis pilosula* seedlings. 2. Head of *Codonopsis pilosula* seedlings. 3. Film edge. 4. Mulch film. 5. Outcrop area.

long, are transplanted to a depth of 50 mm with a spacing of 45 mm between plants. Each seedling is tilted at a 15° angle, and rows are spaced 300 mm apart. The theoretical plant density is 444,450 plants per hectare. The film-covered outcrop has a width ranging from 0 to 40 mm. A black plastic film, 300 mm wide and 0.01 mm thick, is used to cover the seedbed, with its edges secured by soil.

Overall structure and main technical parameters

As shown in Fig. 3, the tilted transplanting machine for *Codonopsis pilosula* comprises a frame, a suspension device, a trenching device, a rotary tiller and soil throwing device, a soil lifting device, a tracked soil conveying device, a seedling throwing device, and a film covering device. Its main technical parameters are listed in Table 1.

Working principle

This machine can perform multiple tasks simultaneously, including trenching, rotary tilling, soil throwing, bed covering, film mulching, and final soil covering. Before operation, seedlings are manually placed on the planting device, ensuring their tops align with the high end of the planting groove. During operation, the transplanter's suspension system connects to the tractor's three-point hitch. The tractor's power output shaft transmits power through the gearbox, driving the rotary tiller and soil thrower. As the machine moves forward, the trencher creates tilted planting grooves in the loosened soil. Simultaneously, the wheels drive the planting device, precisely placing the *Codonopsis pilosula* seedlings into the seedbed. The soil lifting device raises soil to the covering device, which uses a conveyor belt to cover the planted seedlings in the groove. Another portion of the soil is diverted through a chute to the soil spreading drum of the film mulching device. Soil then flows out from both sides of the soil compression drum, covering the edges of the film.

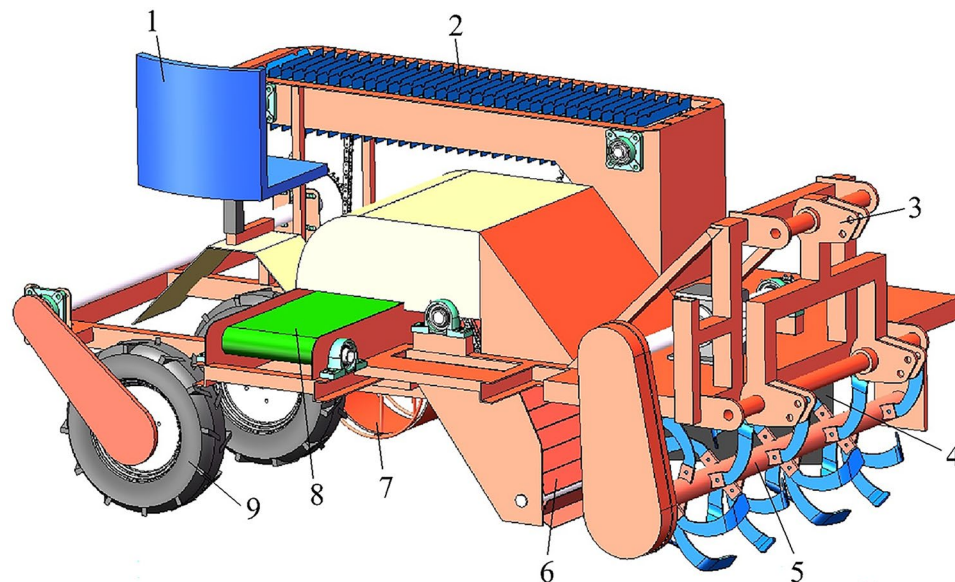


Figure 3. Overall layout of the machine. 1. Seat. 2. Seedling feeding device. 3. Suspension device. 4. Furrower. 5. Rotary tiller and soil throwing device. 6. Scraper type soil lifting device. 7. Film coating device. 8. Crawler type soil conveying device. 9. Ground wheel.

Machine parameters	Numerical values
length × width × height [mm]	2480 × 1735 × 1225
PTO power required	25.7 kw
Overall mass	537 kg
Seedling delivery method	Artificial seeding
Row spacing	45 mm
Operating speed	0.1–0.2 m/s
Productivity	0.12–0.24 ha/h
Number of transplanting rows	1
Tilt angle	15°
Plastic film width	300 mm

Table 1. Main technical parameters of transplanting machine.

Compared to the traditional method of manually inserting seedlings into the planting ditch while digging, the leakage rate is relatively high. The seedling feeding device of this design adopts a ground wheel belt dynamic chain transmission method. The seedling groove is installed on the chain, and the seedlings are neatly placed on the groove by manual labor while the unit moves forward. The spacing between each two seedling grooves is fixed, and the chain transports the seedling groove to the lowest point and freely falls off to the seedling bed, ensuring that the distance between the seedlings is not affected by the overall forward speed of the machine, keeping the distance between the seedlings stable while reducing the leakage rate.

Main working component design

Rotary tiller and soil throwing device

The rotary tiller and soil throwing device are the main working components of the party *Codonopsis pilosula* oblique transplanting machine. Figure 4 is a schematic diagram of the principle and structure of rotary tillage and soil throwing. When working in the field, the power takeoff shaft (PTO) of the tractor transfers power to a gearbox. After the gearbox changes speed, the power is transmitted to the rotary tiller shaft through a chain transmission. The rotary tiller shaft drives the tines mounted on the rotary tiller shaft which cut the soil axially and also throw the soil to the rear, providing soil for a scraper type soil lifting device to ensure the covering operation of the seedbed and film surface.

A Cartesian coordinate system has been established with the origin O positioned at the center of the rotary tiller's axis. The positive x-axis direction aligns with the unit's forward movement, while the positive y-axis points vertically upwards¹⁵. The tines of the rotary tiller rotate around the origin, and a reference point is selected at the maximum radius of a tine tip. Figure 4 illustrates the trajectory of the reference point during operation.

By treating working time t in seconds as the variable parameter, the equations of the tip of the rotary tiller tine trajectory can be written as:

$$\begin{cases} x = v_m t + R \cos(\omega t) \\ y = R \sin(\omega t) \end{cases} \quad (1)$$

where R is the maximum turning radius of the rotary tiller tine endpoint (mm); ω is the rotation speed of the rotary tiller in rad/s, and v_m is the forward speed of the machine in m/s.

Using the ratio λ of the rotary tiller tangential speed and planter forward speed:

$$\lambda = \frac{R\omega}{v_m} \quad (2)$$

the equations of the tine tip trajectory becomes:

$$\begin{cases} x = R \left(\frac{\omega t}{\lambda} + \cos \omega t \right) \\ y = R \sin(\omega t) \end{cases} \quad (3)$$

For different rotary tiller speed ratios λ , the trajectory of the tip of the rotating tines will change. The soil after cutting will also follow different trajectories, so the speed ratio λ will also affect the soil throwing operation.

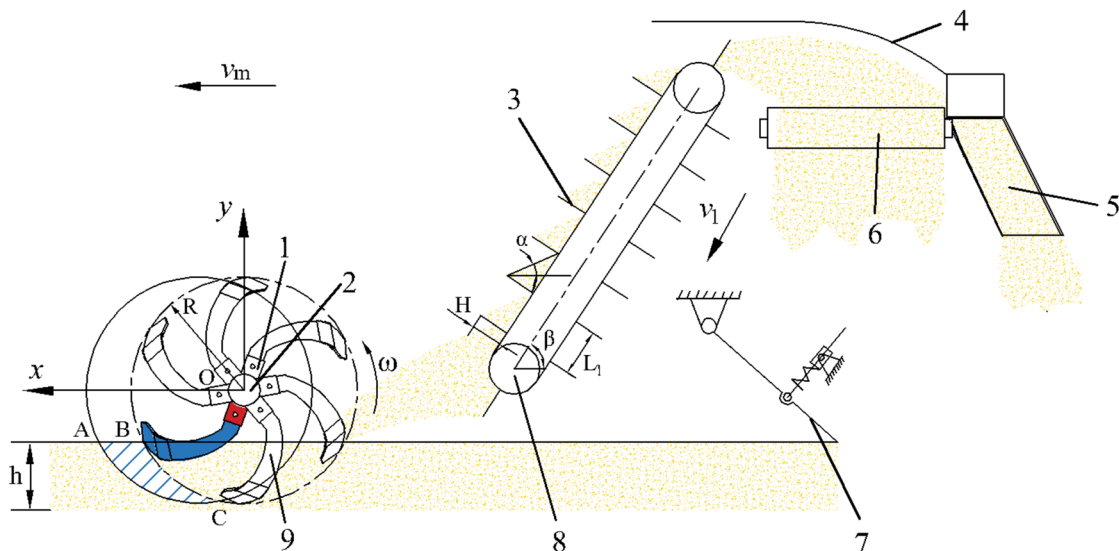


Figure 4. Schematic diagram of the principle of rotary tillage and soil throwing. 1. Rotary tiller tine holder. 2. Rotary tiller shaft. 3. Scraper. 4. Cover piece. 5. Soil chute. 6. Crawler type soil conveying device. 7. Film covering device. 8. Chain wheel. 9. Rotary blade.

Depending on λ , the trajectory of the tine tip as the rotary tiller moves forward will have three different shapes as shown in Fig. 5.

The rotary tiller tine first cuts the soil, then throws the soil backwards. Through graphical analysis, it is found that only when $\lambda > 1$ and the trajectory is a trochoid, the tine can satisfy the condition of throwing soil backwards. Additionally, for larger the speed ratios λ , the unit volume soil will be cut by the tines multiple times, resulting in a better soil fragmentation. This is beneficial for increasing the amount of soil thrown backwards by the rotary tiller and soil throwing device, and that the bottom of the cut soil will also be smoother. This basic action requires the rotary tiller tine to meet the normal working conditions of the rotary tiller throwing device from the beginning of entering the soil to the end of throwing the soil and lifting it off the ground. The derivative of the above formula is calculated, and the velocity equation at the tip of the rotary tiller tine is obtained as follows¹⁶.

$$\begin{cases} v_x = \frac{dx}{dt} = \frac{R\omega}{\lambda} - R\omega \sin(\omega t) \\ v_y = \frac{dy}{dt} = R\omega \cos(\omega t) \end{cases} \quad (4)$$

The magnitude of the velocity at the tip of the rotary tiller tine will therefore be:

$$v = \sqrt{v_x^2 + v_y^2} = \frac{R\omega}{\lambda} \sqrt{1 - 2\lambda \sin(\omega t) + \lambda^2} \quad (5)$$

To meet the condition of backward soil throwing, the horizontal component of the velocity of the tip of the tine at any point of its trajectory must point backwards i.e.

$$v_x = \frac{R\omega}{\lambda} - R\omega \sin(\omega t) < 0 \quad (6)$$

For $\sin(\omega t) = R/(R-h)$ where h is the depth of cultivation see in Fig. 4 we get

$$h < R \left(1 - \frac{1}{\lambda} \right) \quad (7)$$

The above formula indicates that the radius R of the end point of the rotary tiller tine, the rotational speed ω and forward speed v_m of the tiller determine the shape of tine tip trajectory and the depth of cultivation h .

During normal operation, the rotary tiller cuts soil in a manner similar to slab milling with a plain milling cutter. This principle involves the sequential engagement and cutting of the soil by tines on the same rotating plane of the cutter shaft, as described in^{17,18}. According to Fig. 4, as the first tine initially cuts into the soil at point A, it rotates and advances forward in a straight line along with the unit. After a specific time interval (t), the second tine, positioned on the same rotational plane, starts entering the soil at point B. The linear distance of AB is the cutting pitch S of the tine which can be calculated as:

$$S = \frac{60v_m}{nz} = 2\pi \frac{R}{\lambda z} \quad (8)$$

where v_m is the forward speed of the implement in m/s; n is the rotational speed of the cutter shaft in rpm, and z is the number of tines mounted in the same rotating plane.

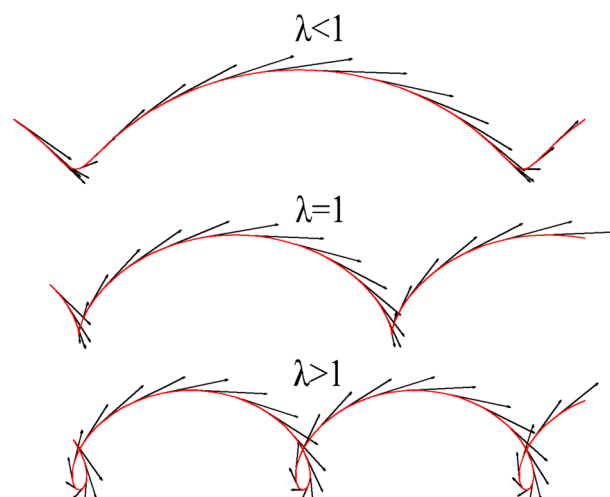


Figure 5. Trajectory of the tine tip for different rotary tiller speed ratios speed ratios λ .

The volume of soil cut by a single tine in one rotation of the rotary tiller can be approximated as the product of the cutting area A_{ABC} and the cutting thickness T ¹⁹:

$$\left\{ \begin{array}{l} A_{ABC} = Sh \\ T = L\sin(\pi - \theta) \end{array} \right. \quad (9)$$

where S is the pitch of soil cutting; h is the depth of cultivation, and L is the cutting length of the rotary tiller tine (all in mm), while θ is the tangent tine bending angle in radians.

The total mass of soil cut by a single rotary tiller tine in one rotation cycle is:

$$M = \rho TA_{ABC} = \rho TSh \quad (10)$$

where ρ is the soil density in kg/m³.

From Eqs. (7), (8), (9), and (10), it can be seen that the mass of soil tilled by the rotary tiller is related to parameters R , ω , L , θ , h , z and v_m . Of these, the rotational angular velocity ω and the tillage depth h are the main factors affecting the amount of soil thrown by the rotary tiller.

Soil lifting—tracked soil conveying device

Figure 6 depicts the main components of the soil lifting and crawler-type soil conveying device. These are the soil lifting scraper, soil lifting cover, crawler-type soil conveying device, soil chute, and power shaft. During operation, the front rotary tiller and soil throwing device cast the cut soil onto the soil lifting device. The soil lifting device tilts at a controlled linear speed to elevate the soil, which then falls onto the crawler-type soil conveying device due to inertia. The crawler then transports the soil, depositing some onto the seedbed from one side and the remaining portion onto the soil compression drum via the soil chute, thereby covering both sides of the film.

Analysis and calculation of soil lifting volume

To guarantee adequate soil coverage over seedlings and film edges during operation, a scraper-lifting chain soil lifting device was designed. This device utilizes an active sprocket, a driven sprocket, a lifting chain, and a scraper. It is installed obliquely at the rear of the rotary tiller's soil throwing device, positioned in the frame's center. The inclination angle is typically kept under 45°. The scraper plate is attached to the chain, and the active sprocket drives the lifting chain to elevate the soil thrown by the rotary tiller. This design offers several advantages, including stable operation, consistent soil lifting quantity, and high lifting efficiency, ultimately contributing to efficient soil transportation.

When the scraper with lifting chains is tilted for lifting, gravity causes the soil between the scraper plates to form a right triangle. According to Fig. 4, the height of the soil on the lifting scraper can be calculated as²⁰:

$$H = L_1 \tan(\beta - \alpha) \quad (11)$$

where $L_1 = 120$ mm is the spacing between two scraper plates; β is the angle between the lifting chain and the horizontal plane (typically 45°), and α is the internal friction angle of the soil. In the arid Northwest region of China, the soil is mainly yellow loess with $\alpha = 28^\circ$. With these values, the calculated soil height on each lifting scraper is $H = 40$ mm.

The lifting speed of the scraper-type soil lifting device significantly impacts its performance, especially when aiming for continuous and uniform soil coverage over seedlings and film edges in planting furrows. If the speed is too high, the large inertia of the flipping motion can cause the soil to fall off the scraper, leading to uneven coverage and reduced effectiveness. Conversely, a slow lifting speed may not deliver enough soil to the covering

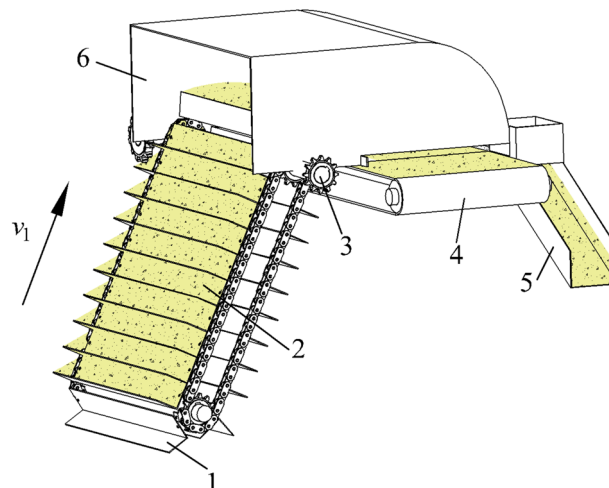


Figure 6. Diagram of soil lifting and tracked soil conveying device. 1. Soil lifting scraper. 2. Soil. 3. Power shaft. 4. Crawler type soil conveying device. 5. Soil chute. 6. Lifting soil cover.

device, resulting in insufficient coverage and potential leaks. The designed soil lifting device has a tilted angle $\beta = 45^\circ$. During operation, it combines two speeds: the forward speed (v_m) of the transplanting machine and the lifting line speed (v_1) of the scraper. This combination determines the overall soil lifting performance. The lifting line speed of the scraper can be calculated with²¹:

$$\begin{cases} v_1 = \frac{Q}{tBH\psi\gamma k} \\ t = \frac{l}{v_m} \end{cases} \quad (12)$$

where B is the width of the scraper (equal to 1000 mm); ψ is the filling coefficient of the scraper lifting device with an average value of 0.86 (typical values of ψ are between 0.75 and 0.97²²), k is the incline coefficient, t is the time in seconds required for the planter to travel 1000 mm; l is the working walking distance of the planter (equal to 1000 mm), and v_m is the forward speed of the planter, equal to 0.1 m/s. According to reference²², for scraper-type soil lifting device with an incline angle of 45°, the incline coefficient k is 0.40. Corresponding to these values, the calculated linear velocity v_1 of the scraper is 0.09 m/s.

The relationship between the planter's forward speed v_m , and the linear speed v_1 of the soil lifting scraper, indicates that when the unit travels 1000 mm, the scraper travels 900 mm. At a spacing of 120 mm, it corresponds to 7 scrapers needed to complete the soil lifting operation when the planter travels 1000 mm. The amount of soil lifted by a single scraper is:

$$Q_{m1} = \rho BS \quad (13)$$

where ρ is the soil density equal to 1300 kg/m³²³ and S is the cross-sectional area of a single scraper, which is the area of each right-angle triangle visible in Fig. 7 i.e.

$$S = \frac{L_1 H}{2} \quad (14)$$

The total amount of soil lifted when the planter travels 1000 mm is:

$$Q_m = 7Q_{m1} \quad (15)$$

Therefore, if the soil lifting capacity Q_{m1} of a single scraper is 3.12 kg, then for 7 scrapers $Q_m = 21.84$ kg.

Analysis and calculation of soil cover

One of the main factors affecting the quality of transplanting machine operation is the amount of soil covered by the track type soil conveying device on the seedbed and film edge. Seedlings need to absorb sufficient water and oxygen to germinate smoothly. Excessive soil coverage on the seedbed can affect soil permeability and water permeability, leading to the inability of seedlings to absorb water and oxygen smoothly, affecting their growth. When the amount of soil covering the edge of the film is insufficient, it is difficult to resist the natural wind force from the outside to peel off the film.

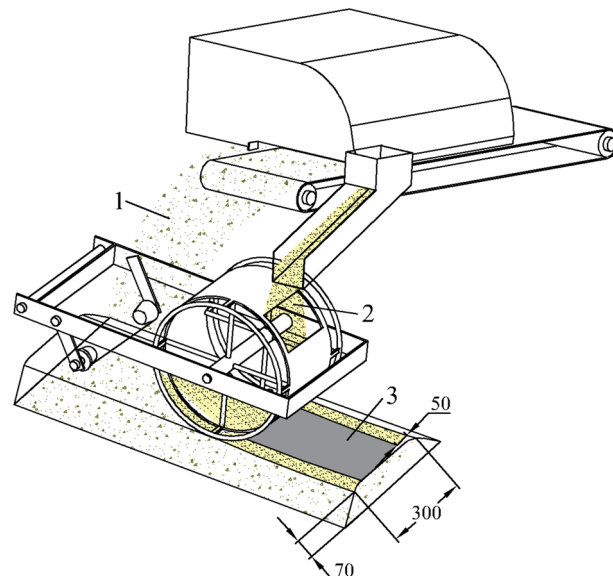


Figure 7. Schematic for soil cover analysis. 1. Soil coverage of seedbed. 2. Soil coverage at the edge of the membrane. 3. Plastic mulch film.

As shown in Fig. 7, in order to evaluate the consistency and stability of the soil covering operation on the seedbed and film edge during transplanting, it is necessary to calculate the amount of soil covering.

The total amount of soil covering for the seedbed and membrane edge by the soil covering device is:

$$Q_n = Q_1 + Q_2 \quad (16)$$

where Q_1 is the amount of soil cover for the seedbed, and Q_2 is the amount of soil covering the membrane edge, both in kg. When calculating these two amounts, it will be assumed that the machine travels 1000 mm. The amount of soil cover is the product of the soil volume in a testing area and the soil density, expressed as:

$$\begin{cases} Q_1 = \frac{1}{2} \rho l B_1 h_1 \\ Q_2 = \rho l B_2 h_2 \end{cases} \quad (17)$$

where $B_1 = 300$ mm is the width of soil cover for the seedbed; $B_2 = 100$ mm is the width of the membrane edge covering soil; $h_1 = 70$ mm is the soil cover thickness of the seedbed; $h_2 = 50$ mm is the thickness of soil covering the membrane edge. With these values, $Q_1 = 13.65$ kg and $Q_2 = 6.5$ kg. Therefore, the theoretical soil cover Q_n required for the transplanting machine to travel 1000 mm is 20.15 kg.

Through analysis and calculation of the amount of soil lifted by the scrapers of the soil lifting device, and the amount of soil required for the film edge of the seedbed, it was found that the amount of soil lifted by the scraper type soil lifting device Q_m is equivalent to the amount of soil required for the soil covering belt Q_n , meeting the soil covering requirements.

Seedling feeding device

The seedling placement process is an important factor in ensuring the quality of operation of the transplanting machine. To ensure that the *Codonopsis pilosula* seedlings are neatly placed in the planting ditch²⁴, it is necessary to design the seedling placement device accordingly. Currently, the commonly used methods for controlling seedling spacing include pre-treatment seedling belt method⁹, hole tray seedling belt method²⁵, and manual seedling feeding method⁷. In the current design, a double row chain drive seedling groove that is installed on the conveyor chain, combined with manual seedling placement were implemented.

As shown in Fig. 8, the seedling feeding device includes a seedling groove, two driving shafts, a driven shaft, a tensioning sprocket shaft, a driving sprocket, two driven sprockets, a tensioning sprocket, and a conveyor chain. The bearings of the driving shaft and of the driven shaft are attached to the frame, while the ground wheels provide power to the driving shaft. The driving shaft rotates and transmits power to the driven shaft through chain transmission, thereby driving the entire seedling feeding device during operate.

Analysis of seedling movement

As shown in Fig. 9, the driven shaft 2 of the seedling feeding device rotates counterclockwise, and the seedling groove moves vertically downwards at a speed v_c driven by the transmission chain. At the same time, the plnter walks at a speed v_m , and the seedlings move with the seedling groove to point O and begin to detach and lands into the planting ditch. The seedling head tribe is located at point P, the root tribe is located at point Q, the horizontal displacement is L , and the vertical displacement is H .

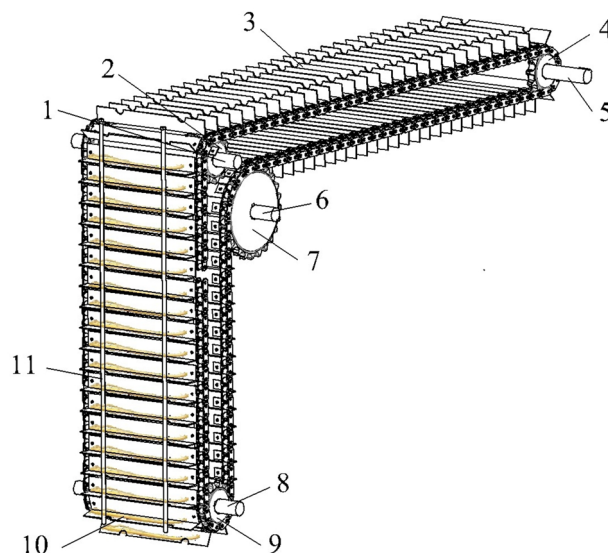


Figure 8. Schematic of the seedling feeding device. 1. Driven shaft 1. 2. Driven sprocket 1. 3. Seedling trough. 4. Driving sprocket. 5. Drive shaft. 6. Tensioning sprocket shaft. 7. Tension sprocket. 8. Driven shaft 2. 9. Driven sprocket 2. 10. *Codonopsis pilosula* seedlings. 11. Seedling blocking rod.

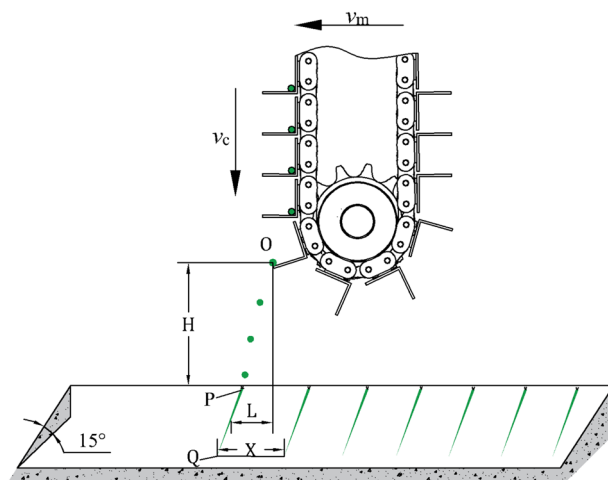


Figure 9. Schematic of seedling deployment process.

As shown in Fig. 10, a Cartesian coordinate system has been chosen with the origin at O where the seedlings leave the seedling trough, the X -axis in the horizontal direction, and the Y -axis in the vertical direction. When the seedlings leave the seedling trough, they are affected by both gravity and air resistance. At the moment of detachment, the seedlings tilt down at the combined speed v_p of the horizontal unit forward speed v_m and the vertical downward chain transmission speed v_c .

The air resistance, which affects the seedling placement, can be calculated with:

$$f = uV_p \quad (18)$$

where f is the air resistance (N); μ is the air resistance coefficient; v_p is the seedling speed (m/s).

The horizontal and vertical accelerations when the seedlings move in the air after leaving the seedling trough are:

$$\begin{cases} a_x = \frac{f_x}{m} \\ a_y = \frac{mg - f_y}{m} \end{cases} \quad (19)$$

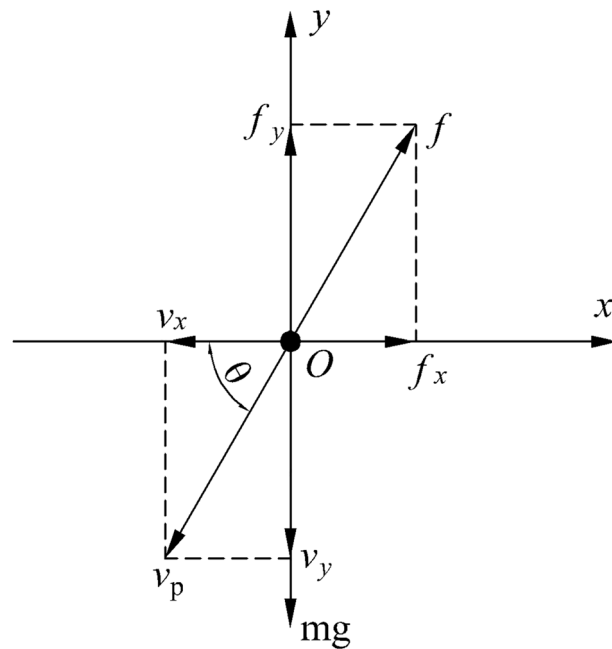


Figure 10. Analysis of force on seedlings at the moment they detach from the seedling groove.

where a_x is the acceleration of the seedlings in the horizontal direction (m/s^2); a_y is the vertical acceleration of the seedlings (m/s^2); f_x is the horizontal component of the air resistance acting on the seedlings (N); f_y is the vertical component of the air resistance acting on the seedlings (N), and g is the gravitational acceleration (m/s^2).

The velocities of seedlings in the X and Y directions when they detach from the seedling groove are:

$$\begin{cases} v_x = v_m \\ v_y = v_c \end{cases} \quad (20)$$

The resultant velocity of seedlings at the moment of detachment from the seedling trough is:

$$v_p = \frac{v_m}{\cos\theta} = \frac{v_c}{\sin\theta} \quad (21)$$

where θ is the angle between the direction of movement and the horizontal direction at the moment of seedling detachment ($^\circ$).

After the seedlings leave the seedling trough, they will be affected by their own gravity. Therefore, the horizontal and vertical movement speeds of the seedlings during the falling process are:

$$\begin{cases} v'_x = v_m \\ v'_y = v_c + gt \end{cases} \quad (22)$$

where v'_x is the horizontal movement speed of the seedlings (m/s); v'_y is the vertical movement speed of the seedlings (m/s) and t is the duration of seedling movement (s).

The horizontal and vertical displacement during the process of seedling falling are:

$$\begin{cases} L = v_m t \\ H = v_c t + \frac{gt^2}{2} \end{cases} \quad (23)$$

Through the analysis of the process of seedling placement, it can be concluded that the horizontal displacement during the seedling falling process is related to the walking speed V_m of the machine, while the vertical displacement during the seedling falling process is related to the chain transmission speed v_c . When the walking speed v_m of the unit, the chain transmission speed v_c , and the seedling height H (the vertical displacement during the seedling falling process) are all determined, the horizontal displacement L during the seedling falling process is a constant value.

Film coating device

Figure 11 is the structural diagram of the laminating device, the film coating device mainly consists of a film hanging frame, a film hanging roller, a connecting rod, a connecting frame, and a soil separation and compaction roller. The entire film covering device is installed on the rack behind the seedling feeding device, which is hinged to have a terrain-like effect. Two film hanging sleeves are hung on both sides of the film to prevent the film from falling off the sleeves. The film hanging sleeves are designed in a circular cone shape, and the film being inserted from the side with a small cross-sectional area. The two film hanging sleeves are symmetrically installed on the film hanging frame, and the film is clamped between the two film hanging sleeves. The soil separation and compaction roller is installed on the connecting frame at the back of the hanging film sleeve, which has the functions of spreading and pressing the film. When the soil separation and compaction roller rolls, it divides the

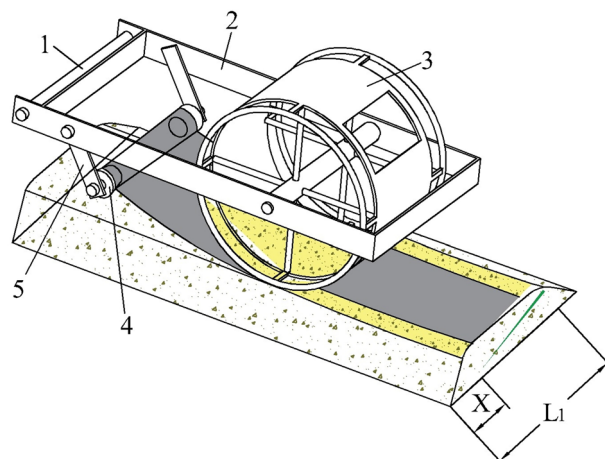


Figure 11. Schematic diagram of the lamination device structure. 1. Connecting rod. 2. Connecting frame. 3. Split soil compaction drum. 4. Hanging film roller. 5. Hanging film rack.

soil to the soil outlets on both sides and covering them on sides of the film edge, improving the quality of film coverage and achieving stability and uniformity of soil coverage on both sides of the film edge^{26–28}.

According to agronomic requirements, the film covering process needs to achieve an exposed effect, so the selection of plastic film should meet the following requirements:

$$L \leq L_1 - X \quad (24)$$

where $L_1 = 350$ mm is the straight-line distance from the seedling head to the ridge; L is the width of the plastic film, equal to 300 mm from agronomic considerations, and $X = 40$ mm is the width of the seedling outcrop.

To meet the agronomic requirements of covering soil on the membrane edge, the relevant parameters of the soil compaction drum need to be determined. The soil compaction drum needs to meet the following requirements:

$$D + 2d = L \quad (25)$$

where $D = 200$ mm is the width of the compaction drum, and $d = 50$ mm is the width of the soil outlet of the soil compaction drum.

Drive system

Figure 12 depicts the transmission system of the machine used for tilted transplanting and plastic-film mulching of *Codonopsis pilosula* medicinal plants. During operation, the transplanting machine's suspension device connects to the tractor's three-point hitch. The tractor's power take-off (PTO) transmits power through the gearbox, driving the rotary tiller and soil lifting devices via a chain transmission system. As the unit moves forward, the trenching device opens a tilted planting ditch in the loosened soil prepared by the rotary tiller. Simultaneously, the ground wheel drives the seedling feeding device's shaft through another chain transmission system. This shaft connects to driven shafts 1 and 2 and the tensioning chain wheel shaft of the seedling feeding device, precisely placing the manually placed *Codonopsis pilosula* seedlings from the seedling slot into the prepared seedbed.

The soil lifting device then transfers soil onto the tracked soil conveying device. Its active shaft connects to the crawler-type soil conveying device. During conveying, part of the lifted soil is transported to the *Codonopsis pilosula* seedbed in the planting ditch, while the remaining portion is diverted through a soil chute onto the film covering device's soil separation drum. The soil then flows out from both sides of the soil separation roller, tightly covering the edges of the film.

To ensure that the agronomic requirements for the spacing between *Codonopsis pilosula* seedlings are met, we need to calculate the transmission ratio of the seedling feeding device. Specifically, if the ground wheel completes one revolution and the driving shaft of the seedling feeding device rotates n times, then the following equation holds:

$$n = \frac{z_1 z_3}{z_2 z_4} \quad (26)$$

where $z_1 = 24$ is the number of teeth on the ground wheel sprocket; $z_2 = 13$ is the number of teeth in the input sprocket of the intermediate shaft; $z_3 = 26$ is the number of teeth on the output sprocket of the intermediate shaft, and $z_4 = 12$ is the number of teeth in the input sprocket of the active shaft of the seedling feeding device.

The ground wheel travels once, and the number of seedlings dropped by the seedling feeding device is:

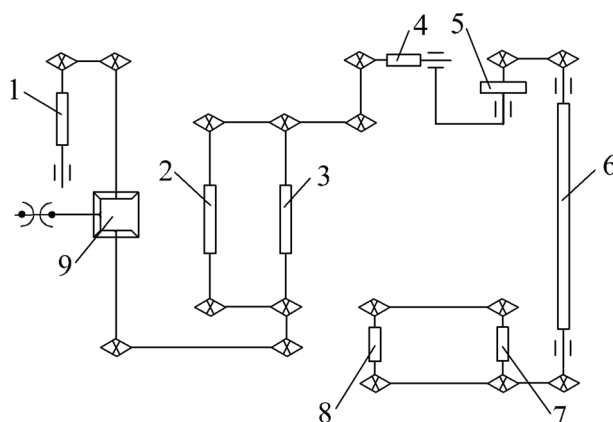


Figure 12. Diagram of transplanting machine transmission system. 1. Rotary tiller axis. 2. Driven shaft of soil lifting device. 3. Active shaft of soil lifting device. 4. Crawler type soil conveying device active shaft. 5. Ground wheel. 6. Intermediate shaft. 7. Active shaft of seedling feeding device. 8. Driven shaft of seedling feeding device. 9. Transmission.

$$m = \frac{n\pi d}{D_1} \quad (27)$$

where $d = 105$ mm is the diameter of the active sprocket of the seedling feeding device, and $D_1 = 40$ mm is the spacing between the seedling blocking plates of the seedling feeding device. The spacing X between plants will therefore be:

$$X = \frac{\pi d_1}{m} \quad (28)$$

where $d_1 = 480$ mm is the diameter of the ground wheel. With the above values, for one ground-wheel rotation, the number of plants planted in each seedling delivery device is $m = 33$ and their spacing $X = 45$ mm.

Simulation of the rotary tillage and soil throwing processes

Simulation parameter settings

To assess the feasibility and performance of the rotary tiller's soil throwing mechanism, the discrete element method (EDEM) was employed to simulate its soil throwing process²⁹. In the simulation, spherical soil particles with a diameter of 8 mm were utilized. The relevant simulation parameters are summarized in Table 2.

The procedure was as follows: In EDEM software, import the SolidWorks models of the rotary tiller throwing device and scraper lifting device. Additionally, create a soil groove model within EDEM with dimensions of 3000 mm (length) \times 1500 mm (width) \times 300 mm (height). Above the soil tank, establish a virtual surface and generate particles from it. Allow these particles to fall freely into the soil tank until it is completely filled.

Simulation process and result analysis

At the beginning of the simulation, the rotary tiller throwing device starts working from one end of the soil groove. The forward speed of the rotary tiller tine is set to 0.4 m/s, the speed is set to 270 rpm, and the total time is set to 7 s. During the simulation process, the rotary tiller tine cuts the soil in a forward rotation, and soil particles are thrown back along the wall of the rotary tiller tine onto the soil lifting scraper. The simulation process is shown in Fig. 13.

Figure 14 shows the simulation and display effect of the stable stage of the rotary tillage soil throwing device. It can be clearly seen that the soil can be thrown onto the soil lifting device and then stably transported.

The amount of soil thrown is the key performance metric of the rotary tiller's throwing device. The rotary tiller tines break up the soil and turn it over, loosening it in the process. As the rotary tiller's throwing device operates, the tines propel the soil back onto the soil lifting scraper. To analyze the throwing performance of the rotary tiller tines, a calculation domain is established above the simulation model. This domain is used to calculate the mass of soil particles that flow through it per unit time during the simulation²⁹. Figure 15 illustrates the behavior of the rotary tiller tine upon entering the soil model. The tine initially throws soil backward, reaching its peak rate at approximately 3 s. Subsequently, the rate stabilizes and exhibits minor fluctuations. Throughout the simulation, the quality of thrown soil roughly matches that of the falling soil. These fluctuations are attributed to a small number of soil particles colliding mid-air. Notably, these collisions do not propel particles outside the simulation domain. While a small fraction of soil particles remains airborne for a brief period, the majority quickly falls onto the soil lifting scraper. Once the scraper reaches capacity, excess soil falls to the ground. The simulation of the rotary tiller and soil throwing device commences at the 4-s mark. By calculating the average value of the stabilized data, we determine that the average mass of soil thrown is 49.44 kg. This value exceeds the soil lifting requirement of the scraper type device, which is 21.84 kg, thereby demonstrating sufficient soil throwing capacity.

Project	Parameter	Numerical value
Soil particle properties	Poisson ratio	0.4
	Shear modulus /Pa	1.0×10^6
	Density/(kg m ⁻³)	1364
Rotary tine properties	Poisson ratio	0.28
	Shear modulus /Pa	3.5×10^{10}
	Density/(kg m ⁻³)	7850
Soil particle-Soil particle interaction	Restitution	0.13
	Static friction coefficient	0.25
	Dynamic friction coefficient	0.30
Soil particle-Rotary tiller tine interaction	Restitution	0.15
	Static friction coefficient	0.50
	Dynamic friction coefficient	0.20

Table 2. Simulation model parameters.

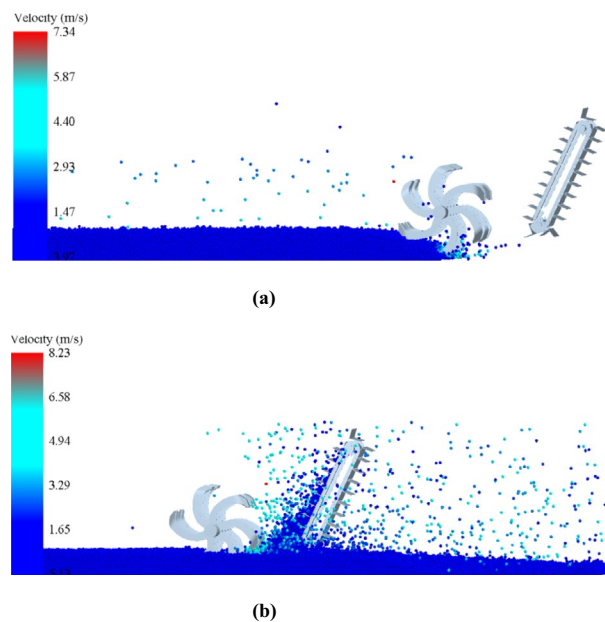


Figure 13. EDEM simulation process. (a) Simulation start run phase; (b) Simulation stable operation phase.

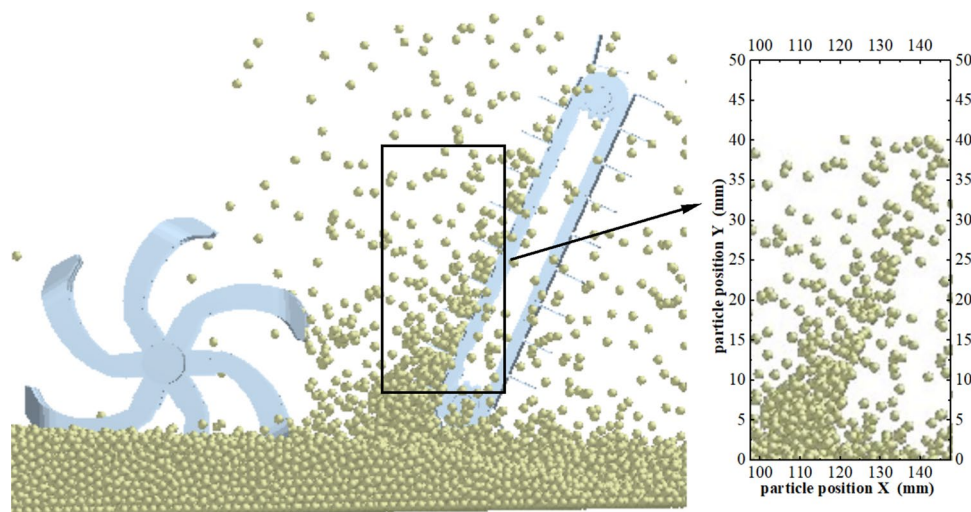


Figure 14. Scraper stabilized soil lifting.

Field experiment

Test conditions and methods

Selecting *Codonopsis pilosula* seedlings with a 6-month seedling cultivation period as experimental seedlings, the average diameter of the seedling head was measured with a vernier caliper to be 3 mm, the average diameter of the seedling root was 3.6 mm, and the average length was 180 mm. Before the experiment, the seedlings were tied with ropes and knots, with an average of 180 plants per bundle. To assess the real-world performance of the designed transplanting machine, field tests were conducted in Chankou Town, Dingxi City, in July 2023. The field experiment is shown in Fig. 16.

To mitigate the influence of ground conditions on the experiment's outcome, the test field was meticulously leveled prior to the commencement of the experiment. The soil composition consisted of yellow loess with a moisture content of 17.1%, a bulk density of 1300 kg/m^3 , and a supporting capacity of 25.7 kW for the machinery. The machine operated in a crawling gear at a forward speed of 0.1 m/s. The average length of the *Codonopsis pilosula* seedlings used was approximately 20 cm, and the target planting depth was set at 5 cm. The target plant spacing was designed to be 4.5 cm. To comprehensively evaluate the planting quality of the prototype, the performance was assessed based on the following parameters established in the JB/T 10291-2013 standard "Standard for Dryland Planting Machinery"³⁰: standard deviation of plant spacing, coefficient of variation of plant spacing, qualified rate of planting depth, qualified rate of planting posture, and qualified rate of outcrop.

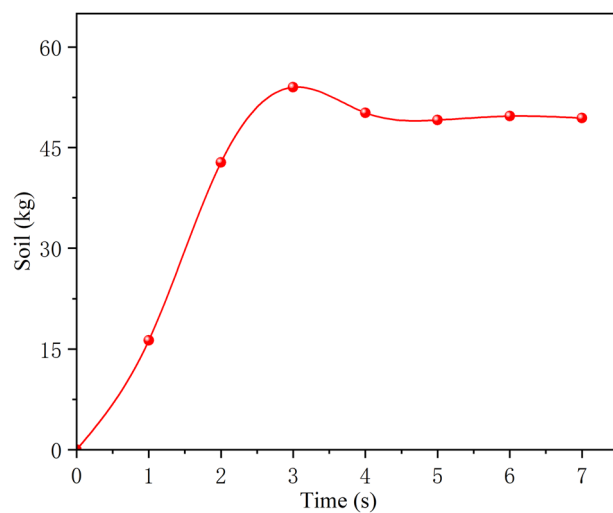


Figure 15. Simulation of soil throwing quality.

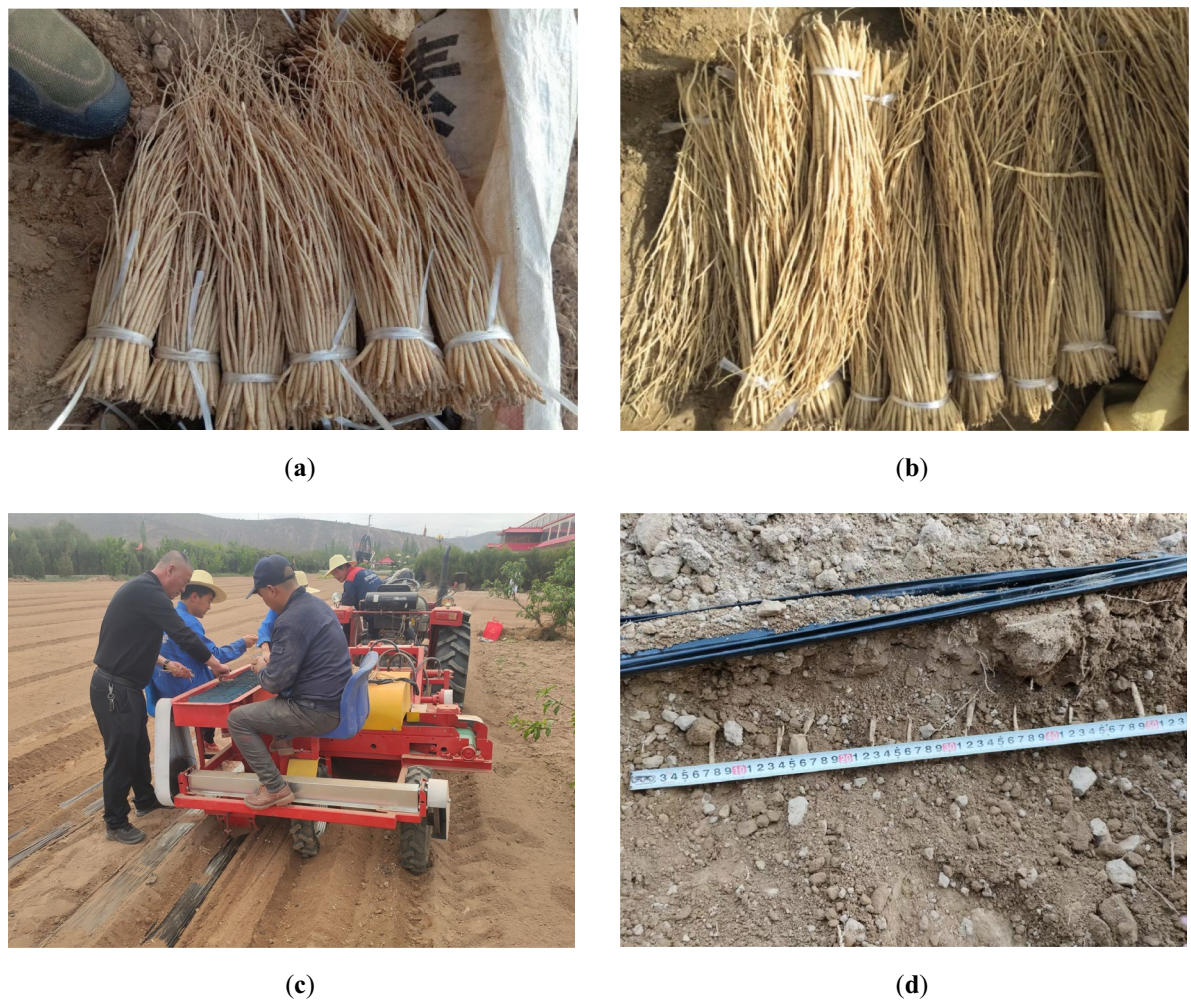


Figure 16. Field experiment. (a) and (b) are *Codonopsis pilosula* seedlings; (c). Prototype test diagram, no co authors can be seen in this picture, can be published; (d) Plant spacing measurement map.

Based on the agronomic requirements for transplanting ginseng seedlings, the planting depth is considered qualified when it falls within the range of 4–6 cm. Similarly, the planting posture is considered qualified when the angle θ between the seedlings and the horizontal plane is between 10° and 20° . Finally, the horizontal distance between the seedling head and the edge of the film is considered qualified when it falls within the range of 3–5 cm. Let N be the total number of measured plants, and let N_1 represent the number of plants with qualified planting depth, N_2 represent the number of plants with qualified planting posture, and N_3 represent the number of plants with qualified outcrop. The qualified rate of planting depth (ε), qualified rate of planting posture (σ), and qualified rate of outcrop (τ) can be calculated using the following formulas:

$$\varepsilon = \frac{N_1}{N} \times 100\% \quad (29)$$

$$\sigma = \frac{N_2}{N} \times 100\% \quad (30)$$

$$\tau = \frac{N_3}{N} \times 100\% \quad (31)$$

By averaging the measurements from 10 randomly selected test areas, we obtained the field performance test results of the prototype shown in Table 3 through calculation, and the results of the plant spacing experiment are shown in Table 4.

Analysis of test results

Field tests demonstrated an average planting depth success rate of 89.50% across 10 testing areas. Similarly, the average planting posture success rate was 84.00%, and the outcrop success rate reached 90%. Plant spacing averaged 4.51 cm with a standard deviation of 0.39 cm and a coefficient of variation of 8.67%. According to JB/T10291-2013 "Standard for Dryland Planting Machinery," acceptable planting depth success rate is at least 80%, and the coefficient of variation for plant spacing should not exceed 20%. These results indicate that the

Test number	Measured number of plants	Number of qualified plants with planting depth	Number of qualified plants in planting posture	Number of qualified plants for membrane side outcrop	Qualified rate of planting depth (%)	Qualified rate of planting posture (%)	Outcrop qualification rate (%)
1	20	19	18	18	95	90	90
2	20	17	17	18	85	85	90
3	20	18	17	19	90	85	95
4	20	18	16	17	90	80	85
5	20	19	16	18	95	80	90
6	20	18	17	18	90	85	90
7	20	17	16	17	85	80	85
8	20	17	16	18	85	80	90
9	20	18	18	19	90	90	95
10	20	18	17	18	90	85	90

Table 3. Prototype field performance test data.

Test number	Average plant spacing (cm)	Standard deviation (cm)	Coefficient of variation (%)
1	4.61	0.46	10.05
2	4.54	0.37	8.15
3	4.35	0.43	9.89
4	4.49	0.29	6.46
5	4.63	0.49	10.58
6	4.55	0.40	8.79
7	4.57	0.41	8.97
8	4.47	0.31	6.94
9	4.39	0.48	10.93
10	4.52	0.27	5.97

Table 4. Plant spacing test results.

prototype met both criteria, ensuring operational quality while fulfilling the tilted transplanting requirements for *Codonopsis pilosula* seedlings.

Conclusions

The *Codonopsis pilosula* sloping transplanting machine was designed to enhance the efficiency and reduce labor requirements for *Codonopsis pilosula* cultivation. Additionally, the machine creates suitable trenches to promote root growth and seedling germination. The prototype's key components were theoretically analyzed, and relevant designs were implemented.

Based on the agronomic needs of oblique *Codonopsis pilosula* transplanting, the structure and working parameters of the rotary tillage and soil throwing device, soil lifting device, tracked soil conveying device, seedling throwing device, and film covering device were determined. The working principle of each core component was analyzed.

The discrete element method simulated the soil throwing process of the rotary tillage and soil throwing device. A calculation domain was established for the simulation model. The results showed that the average mass of soil thrown was 49.44 kg, while the scraper-type soil lifting device required a lifting amount of 21.84 kg, demonstrating sufficient capacity for soil throwing.

Field experiments conducted in 10 test areas revealed an average qualified rate of 89.50% for planting depth, 84.00% for planting posture, and 90% for outcrop of the Party ginseng seedbed film tilted transplanting machine. The average planting depth and the coefficient of variation for planting spacing both met the standard requirements, ensuring high-quality operation while effectively fulfilling the requirements for tilted transplanting of *Codonopsis pilosula* seedlings.

Data availability

Data are reported within the article.

Received: 8 May 2024; Accepted: 23 July 2024

Published online: 27 July 2024

References

1. Fang, H. L. Establishment of *Codonopsis pilosula* industrial technology innovation strategic alliance in Gansu Province. DailyGanws.com—Gansu Economic Daily (2018).
2. Liu, D. J. *et al.* EDEM simulation study on the performance of a mechanized ditching device for *Codonopsis pilosula* planting. *Agriculture* **12**, 1238 (2022).
3. Chang, Y. High-yield cultivation technology of *Codonopsis pilosula* in Tongwei County. *J. Gansu Agric.* **16**, 68–70 (2014).
4. Yuan, T. *et al.* Design and experiment of a composite seedling picking mechanism with air blowing and vibration for vegetable transplanters. *J. Agric. Mach.* **50**(10), 80–87 (2019).
5. Cui, W. Development of ZFS-1A multifunctional tobacco seedling transplanting machine. Shandong Agricultural University (2013).
6. Xu, G. W. *et al.* Design and experiment of inclined transplanting mechanism for *Salvia miltiorrhiza* on film. *J. Agric. Mach.* **50**(02), 78–89 (2019).
7. Hu, L. L. *et al.* Design and experiment of 2ZGF-2 compound planting machine for sweet potato. *J. Agric. Eng.* **32**, 8–16 (2016).
8. Wang, X. J. *et al.* Design and experiment of a tilted transplanting and trenching device for licorice. *J. Agric. Eng.* **32**(13), 16–23 (2016).
9. Wu, G. W. *et al.* Design and test based on pretreatment of seedlings with bare sweet potato seedling transplanting machine. *J. Agric. Mach.* **53**, 99–109 (2022).
10. Ma, X. L., Zhang, L. H., Liu, P. X. & Li, S. L. Analysis of the current situation and benefits of mechanized cultivation of *Codonopsis pilosula* in Gansu. *Agric. Mach. Technol. Promot.* **240**(10), 29–31 (2022).
11. Dong, W. L., Zhang, L. H., Yang, X. P. & Shan, G. Design and experiment of *Codonopsis pilosula pilosula* transplanter. *Xinjiang Agric. Mech.* <https://doi.org/10.13620/j.cnki.issn1007-7782.2023.02.006> (2023).
12. Wang, J. Z., Sun, W., Wang, H. C., Zhang, H. & Liu, X. L. Design and experiment of a ridge covered plastic film seedling transplanting machine for *Codonopsis pilosula pilosula* seedlings. *Agric. Res. Arid Areas* **03**, 289–298 (2020).
13. Wu, J. *et al.* Design and experiment of 2ZY-6 rapeseed carpet seedling transplanter. *J. Agric. Mach.* **51**(12), 95–102 (2020).
14. Zhang, L. H. Technical promotion of mechanized production of traditional Chinese medicine in Gansu. *Agric. Mach. Market.* **383**(02), 29–31 (2021).
15. Xun, X. L. *et al.* Design and experiment of a rotary blade type flat stubble cutting device for Wang Cao harvester. *J. Agric. Mach.* **53**(05), 112–124 (2022).
16. E, Z. Optimization and discrete element simulation study on the arrangement of reverse rotary tillage knives [D]. Xihua University. <https://doi.org/10.27411/d.cnki.gscg.2019.000343> (2019).
17. Fang, H. M. *et al.* Analysis of soil motion behavior during rotary tillage based on discrete element method. *J. Agric. Mach.* **47**, 22–28 (2016).
18. Zheng, K. *et al.* Design and experiment of axial soil levelling cutter roller with gradual spiral lifting angle for furrow rotiller. *J. Agric. Mach.* **52**, 63–73 (2021).
19. Yan, J. C., Li, H. C. & Hu, J. P. Research on the calculation of the distribution of revealed soil volume in reverse rotary tillage. *Agric. Mech. Res.* **36**(11), 29–33 (2014).
20. Dai, F. *et al.* Design and test of micro ridge film and soil covering joint operating machine. *J. Agric. Mach.* **51**(03), 97–105 (2020).
21. Dai, F. *et al.* Design and experiment of a full film soil covering potato sowing combined machine. *J. Agric. Mach.* **48**(03), 76–83 (2017).
22. China Academy of Agricultural Mechanization Science. *Agricultural Machinery Design Manual* Vol. 2 (China Agricultural Science and Technology Press, 2007).
23. Sun, W. *et al.* Design and experiment of a double handle multi rod potato film punching planting machine. *J. Agric. Eng.* **34**(08), 34–42 (2018).
24. Shi, B. H. *et al.* Design and experiment of the combined machine for transplanting outcrop of *Codonopsis pilosula* with micro ridge covered with film. *Appl. Sci.* **13**(16), 9149 (2023).
25. Hu, M. J. *et al.* The effect of transplanting hole tray seedlings with degradable bowls on the growth characteristics of chili peppers. *Chin. J. Agric. Mach. Chem.* **41**(09), 57–62 (2020).

26. Ma, S. *et al.* Development of a single-sided impeller rotary grape vine soil buried cleaning machine. *J. Agric. Eng.* **34**(23), 1–10 (2018).
27. Liao, Q. X., Du, W. B., Zhang, Q. S., Lin, J. X., Chen, Z. L. & Zhang, J. Q. Design and experiment of adjustable ridge forming and film laying machine for cigar and tobacco leaves seedlings. *J. Agric. Mach.* **66**(01), 1–13 (2022).
28. Sun, W. *et al.* Soil cover characteristics of scraper lifting belt membrane overlying device. *J. Mech. Eng.* **52**(07), 38–45 (2016).
29. Chen, X. Y., Shi, Y. L. & Chen, M. D. Simulation experiment on the soil throwing performance of the rotary tiller blade of a sweet potato ridger based on the discrete element method. *J. Agric. Eng.* **11**(02), 117–120 (2021).
30. JB/T 10291–2013; Dry Land Planting Machinery. Ministry of Industry and Information Technology of the People's Republic of China: Beijing, China, 2013.

Author contributions

Conceptualization, W.S. and M.Z.; software, W.L. and P.A.S.; investigation, W.L., W.S., M.Z. and J.W.; resources, W.S. and P.A.S.; writing—original draft preparation, W.L.; writing—review and editing, W.S., P.A.S., M.Z., J.W. and W.L.; supervision, M.Z., J.W. and P.A.S.; project administration, W.S.; funding acquisition, W.S. All authors have read and agreed to the published version of the manuscript. All participants have been informed and agreed to publish.

Funding

This research was funded by the Gansu Province Agricultural Machinery Equipment Shortcomings Action Project (njyf2024-3-1), the Modern Silk Road Cold and Drought Agricultural Technology Support Project (GSLK-2022-12) and the Gansu Provincial University Industry Support Plan (2024CYZC-33).

Competing interests

The authors declare no competing interests.

Additional information

Correspondence and requests for materials should be addressed to W.S.

Reprints and permissions information is available at www.nature.com/reprints.

Publisher's note Springer Nature remains neutral with regard to jurisdictional claims in published maps and institutional affiliations.



Open Access This article is licensed under a Creative Commons Attribution-NonCommercial-NoDerivatives 4.0 International License, which permits any non-commercial use, sharing, distribution and reproduction in any medium or format, as long as you give appropriate credit to the original author(s) and the source, provide a link to the Creative Commons licence, and indicate if you modified the licensed material. You do not have permission under this licence to share adapted material derived from this article or parts of it. The images or other third party material in this article are included in the article's Creative Commons licence, unless indicated otherwise in a credit line to the material. If material is not included in the article's Creative Commons licence and your intended use is not permitted by statutory regulation or exceeds the permitted use, you will need to obtain permission directly from the copyright holder. To view a copy of this licence, visit <http://creativecommons.org/licenses/by-nc-nd/4.0/>.

© The Author(s) 2024